Supplementary Information for

All-Solid-State Proton-Based Tandem Structure Achieving Ultrafast Switching Electrochromic Windows

Zewei Shao[1,2,#], Aibin Huang[1,2,#], Chen Ming[1,2,#], John Bell[3], Pu Yu[4], Yi-Yang Sun[1,2,*], Liangmao Jin[5], Liyun Ma[5], Hongjie Luo[6,*], Ping Jin[1,2,7] and Xun Cao[1,2,*]

[1]State Key Laboratory of High Performance Ceramics and Superfine Microstructure, Shanghai Institute of Ceramics, Chinese Academy of Sciences, Shanghai 201899, China

[2]University of Chinese Academy of Sciences, Beijing 100049, China

[3]Chemistry, Physics and Mechanical Engineering Science and Engineering Faculty, Queensland University of Technology, Brisbane, Queensland 4001, Australia

[4]State Key Laboratory of Low Dimensional Quantum Physics and Department of Physics, Tsinghua University, Beijing 100084, China.

[5]State Key Laboratory of Advanced Technology for Float Glass, Bengbu, Anhui 233000, China

[6]School of Materials Science and Engineering, Shanghai University, Shanghai 200444, China

[7]Materials Research Institute for Sustainable Development, National Institute of Advanced Industrial Science and Technology, Nagoya 463-8560, Japan

Table S1. Optical modulation, coloration time, bleaching time, and coloration efficiency of various reported ECDs using PEDOT or PEDOT:PSS. In these studies, instead of a proton source, PEDOT:PSS serves as an electrode or an electrochromic layer only. The EC performances of these works are also listed.

Materials	Function	T_c (s)	T_b (s)	ΔT (%)	CE (cm^2/C)	Ref.
PEDOT	EC layer	~	~	54%	183	1
PEDOT	EC layer	~	~	71%	193	2
PEDOT/graphene/Ag NW	EC layer	4.1	3.4	~	~	3
WO_3-PEDOT:PSS	EC layer	2.4	0.8	85.7%	68.8	4
PEDOT:PSS	Electrodes	~	~	~	~	5
grid/PEDOT:PSS	Electrodes	12.7	15.8	70%	108.9	6

References:

1. C. L. Gaupp *et al.*, Composite Coloration Efficiency Measurements of Electrochromic Polymers Based on 3, 4-Alkylenedioxythiophenes. *Chemistry of Materials*, **14**, 3964-3970 (2002).
2. E. Poverenov *et al.*, Major Effect of Electropolymerization Solvent on Morphology and Electrochromic Properties of PEDOT Films. *Chemistry of Materials*, **22**, 4019-4025 (2010).
3. B. Deng *et al.*, Roll-To-Roll Encapsulation of Metal Nanowires between Graphene and Plastic Substrate for High-Performance Flexible Transparent Electrodes. *Nano Letters*, **15**, 4206-4213 (2015).
4. G. Cai *et al.*, Direct Inkjet-Patterning of Energy Efficient Flexible Electrochromics. *Nano Energy*, **49**, 147-154 (2018).
5. R. Singh, R *et al.*, ITO-Free Solution-Processed Flexible Electrochromic Devices Based on PEDOT: PSS As Transparent Conducting Electrode. *ACS Applied Materials & Interfaces*, **9**, 19427-19435 (2017).
6. G. Cai *et al.*, Inkjet Printed Large Area Multifunctional Smart Windows. *Advanced Energy Mate*rials, **7**, 1602598 (2017).

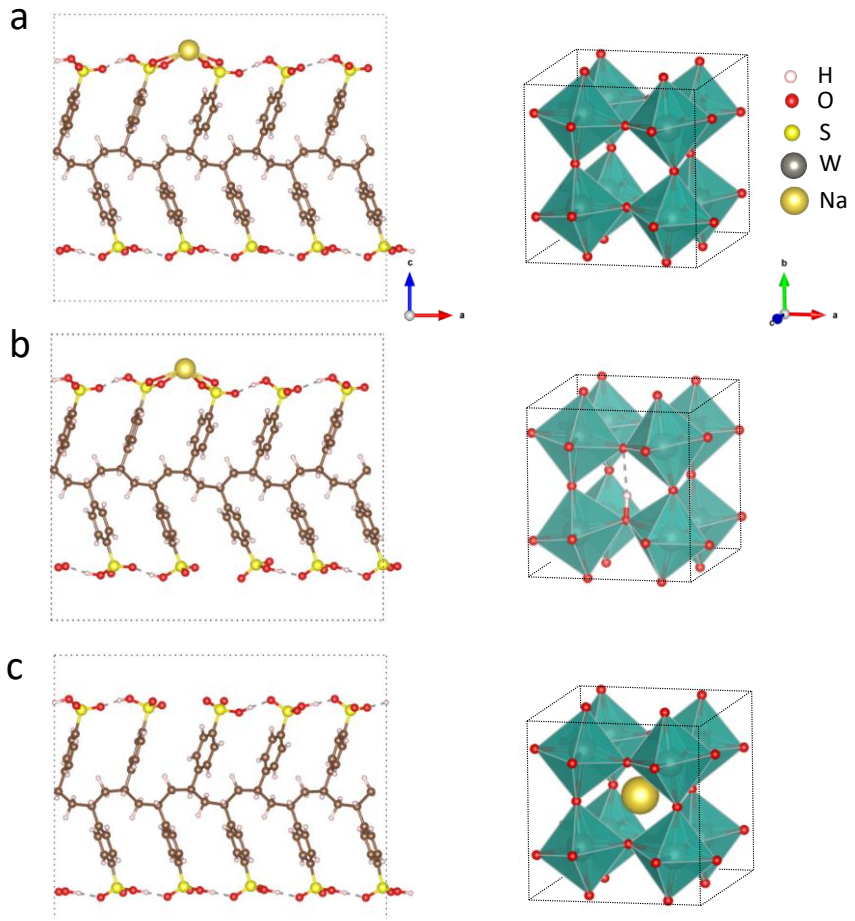

Figure S1. First-principles calculation of atomic structures and energy of proton and Na ions in PSS and WO_3. (a) The proton and Na ions were both adsorbed on PSS leaving a pristine WO_3. (b) One proton was transferred from PSS to WO_3. (c) The Na ion was transferred from PSS to WO_3. The crystalline WO_3 with a monoclinic structure (ICSD#80057) was used to model the amorphous WO_3 which contains 48 atoms. A single PSS chain with five repeating unit was used to model the structure of PSS. Periodical boundary conditions were applied on all the structures.

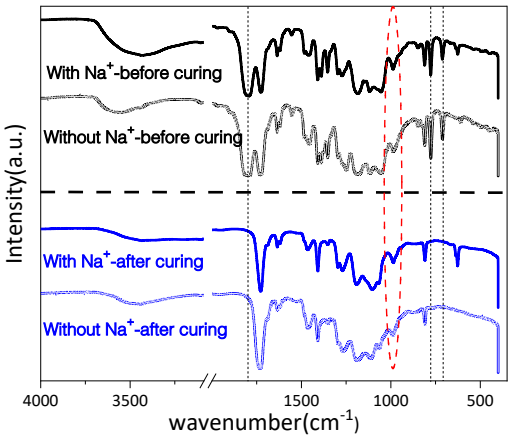

Figure S2. FT-IR spectra of the solid polymer electrolyte. The four curves present four samples with/without Na^+ before/after UV curing. Dotted vertical lines indicate the disappearing peaks after curing. Red dashed circle highlights the slight shift of the peak to the right after inserting Na^+ ions. The red heart indicates a new peak appeared after the inserting the Na^+ ions. The typical stretching and bending peaks of CH_2 at 1460 cm^{-1} and also the stretching peak of the carbonyl group at 1740 cm^{-1} show no obvious change before and after curing. The disappeared peak at 1801 cm^{-1} could be attributed to solvent evaporation.

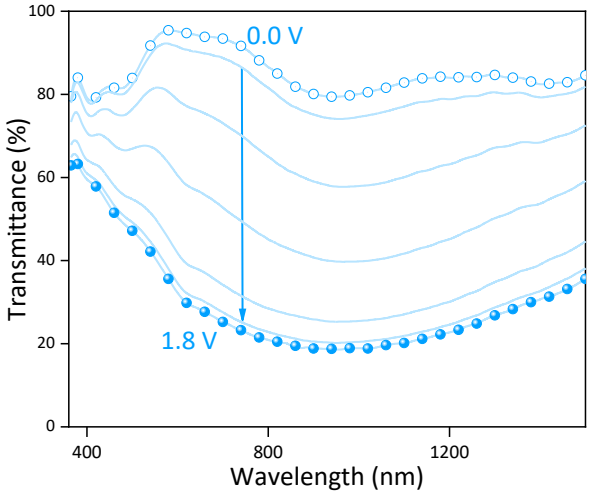

Figure S3. Transmittance spectra of SPE-WO_3 device at voltages from 0 to 1.8 V with a separation of 0.3 V.

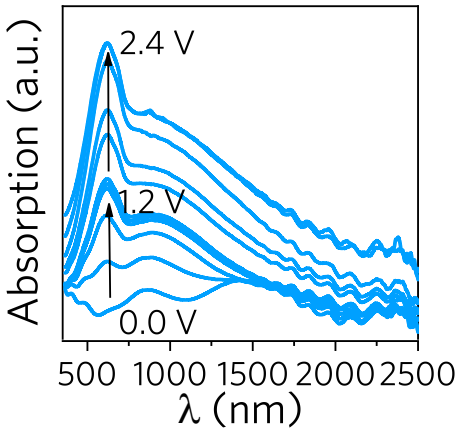

Figure S4. Absorption spectra of SPE/PEDOT:PSS/WO_3 tandem structure device from 0 V to 2.4 V. The absorption peaks are mainly located at 620 and 860 nm consistent with the transmittance measurements.

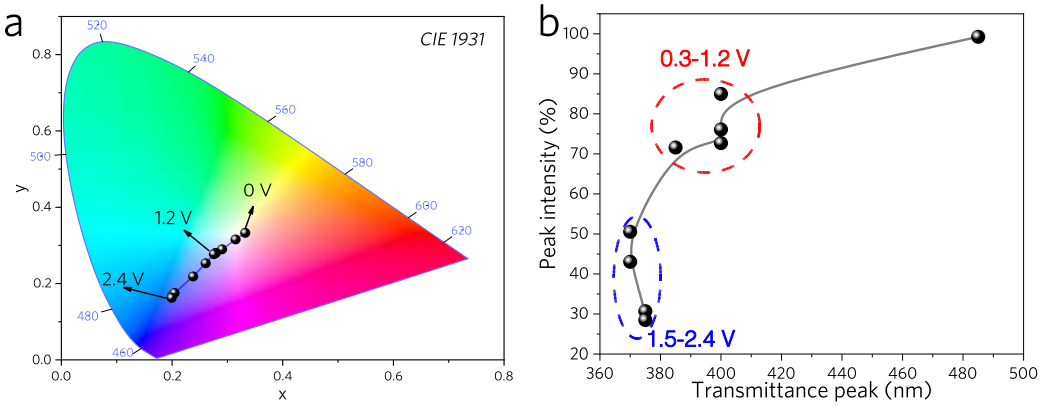

Figure S5. Color changes in the coloration process. (a) peak*x*y* color space (CIE 1931) results of all-solid-state device under different applied potentials (0.0 V to 2.4 V). (b) Peak positions of all-solid-state device under different applied potentials. The EC device absorbs mainly blue light, exhibiting a flatter transmittance in the visible light region. Besides, the coloration process also experiences a two-step change. The coloration peak changes from 400 to 380 nm, which is consistent with the transmittance spectrum.

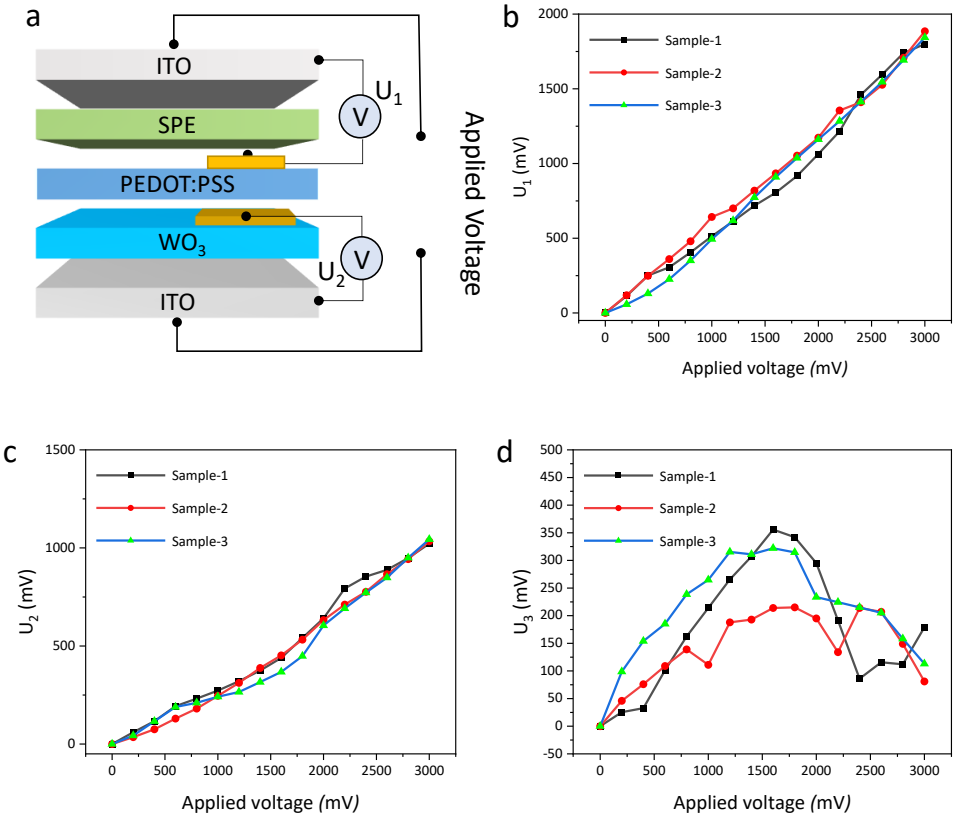

Figure S6. Voltage drops at individual layers on three different samples. (a) Schematic diagram of measurements of the voltage drops. (b) and (c) show the voltage drops on the SPE (U_1) and WO_3 (U_2) layers, which are measured directly, and (d) shows the voltage drop on the PEDOT:PSS layer (U_3), which is obtained by taking the difference between the applied voltage and the sum of U_1 and U_2.

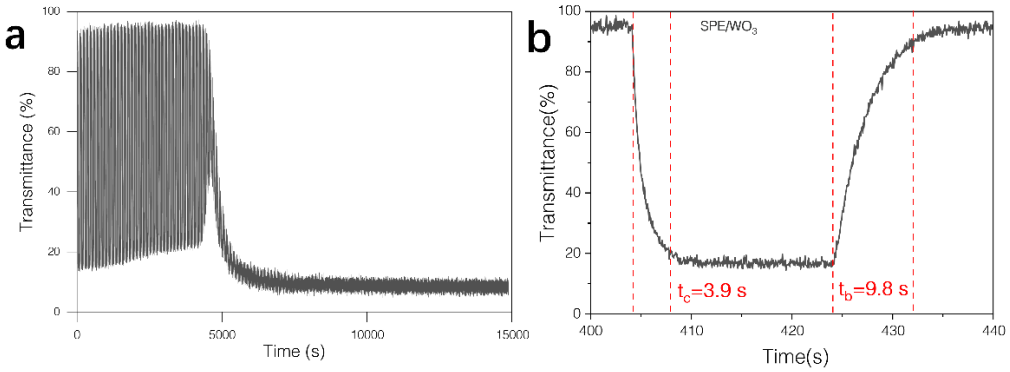

Figure S7. Cycle performance and switching speed of the SPE/WO_3 device without the PEDOT:PSS layer. (a) Real-time transmittance spectra at 670 nm in the −0.5 to 1.5 V window; (b) Switching time measurement. The coloration and bleaching time (switching over 90% of the dynamic range) is about 3.9 and 9.8 seconds. The device degraded quickly after 100 cycles.

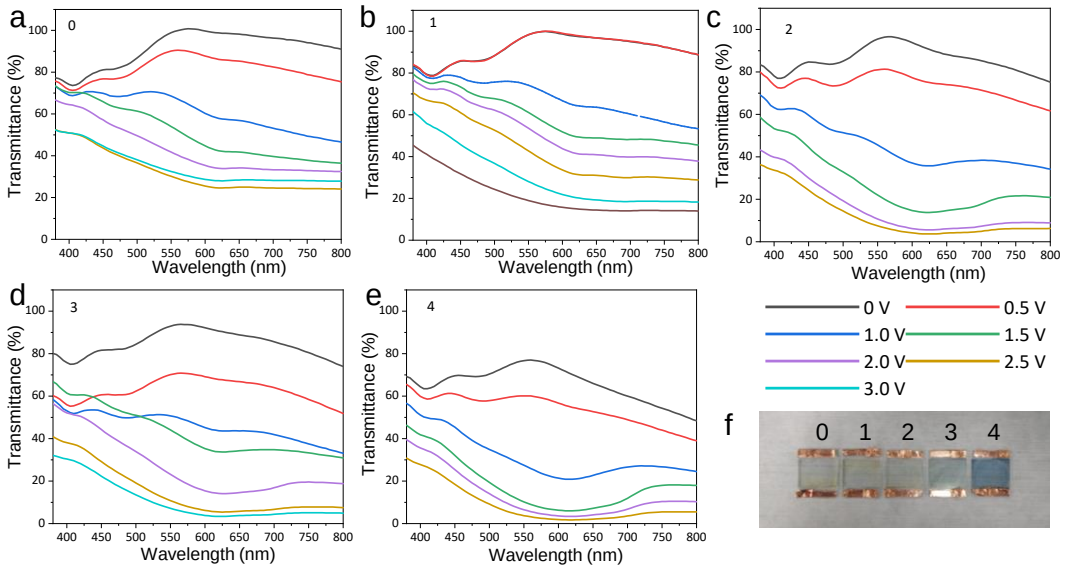

Figure S8. Transmittance spectra and photos of the devices with different thickness of PEDOT:PSS at applied voltages from 0 V to 3 V. The thickness was controlled by the times of spin coating of PEDOT:PSS (a) without PEDOT:PSS, (b)-(e) 1-4 times of spin coating. (f) Photographs of the devices.

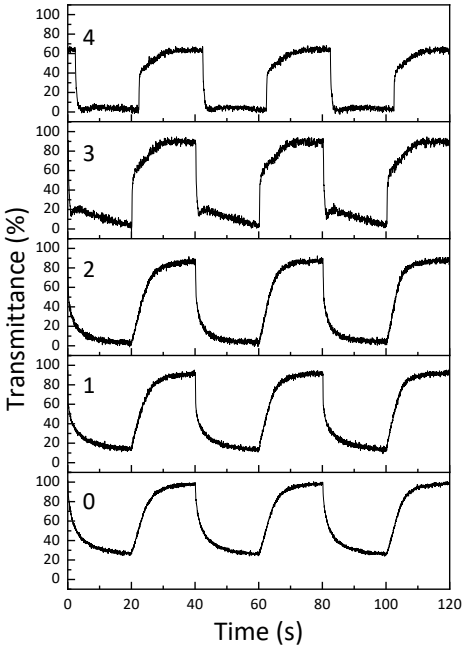

Figure S9. Dependence of switching speed on the thickness of PEDOT:PSS layer. 0-4 corresponds to the devices shown in Figure S4.

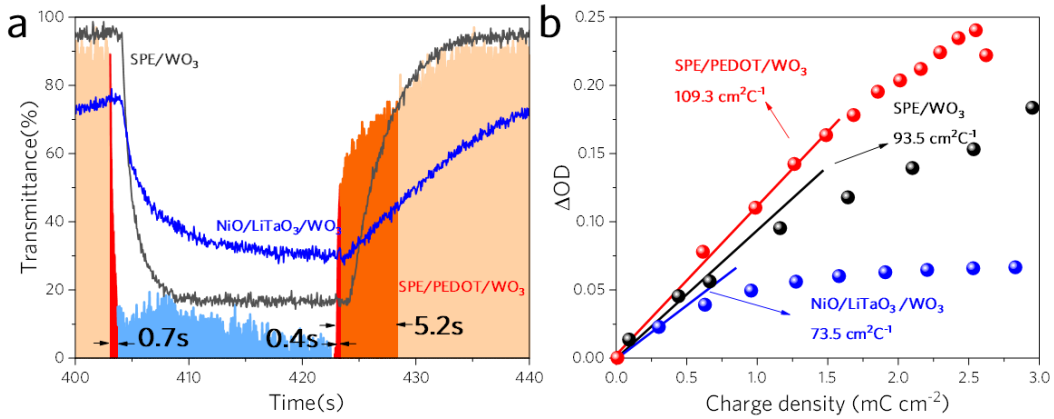

Figure S11. Performance comparison of ECDs with SPE/WO_3, NiO/$LiTaO_3$/WO_3 and the newly designed SPE/PEDOT/WO_3 structures. (a) Switching times from the transmittance spectra. (b) Changes in optical density (ΔOD) at 670 nm with respect to injected charge density. The calculated CEs are 109 cm^2 C^{-1} at 670 nm compared to the 73.5 cm^2 C^{-1} using traditional $LiTaO_3$ electrolyte and 93.5 cm^2 C^{-1} using SPE/WO_3.

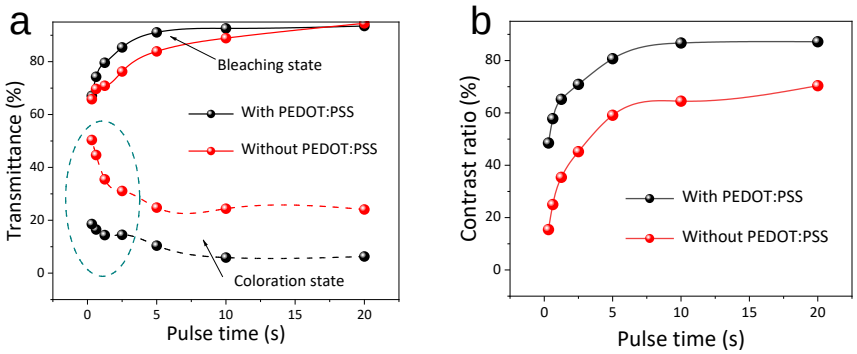

Figure S12. (a) Transmittance vs. voltage pulse width of the devices with and without PEDOT:PSS layer in the coloration and bleaching states. (b) Contrast ratio of the devices under different pulse width.

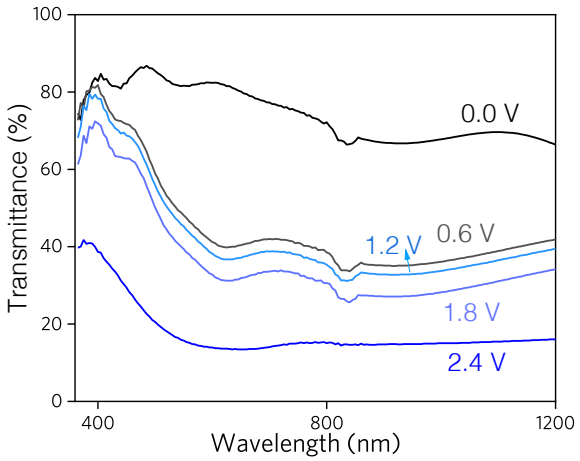

Figure S13. Transmittance spectra of the 10×10 cm^2 EC device using the tandem structure.

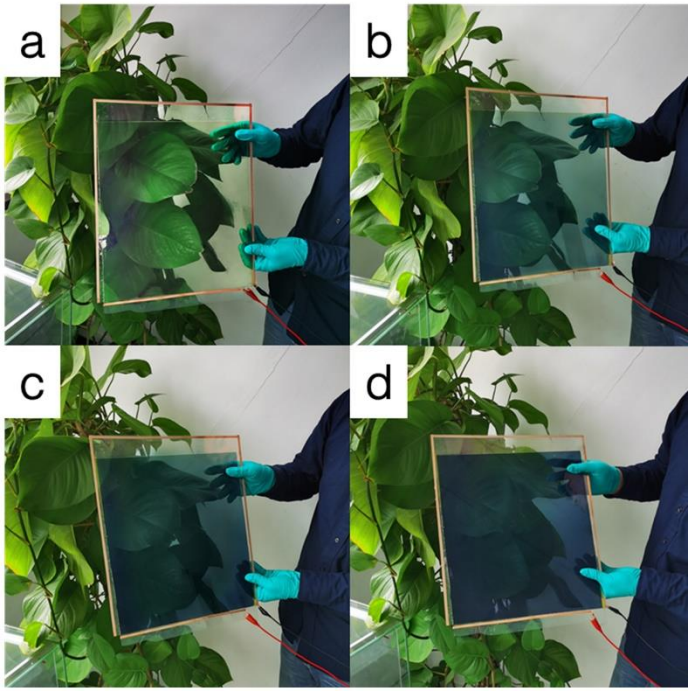

Figure S14. Photographs of the 30 × 40 cm^2 EC device using the tandem structure under (a) 0, (b) 2.0, (c) 4.0, and (d) 6.0 V.